HTML ABSTRACT + LINKS

A uniform glow discharge plasma source at atmospheric pressure

Se Youn Moon and W. Choe[a)]
Department of Physics, Korea Advanced Institute of Science and Technology, 373-1 Guseong-dong, Yuseong-gu, Daejeon, 305-701, Korea

B. K. Kang
PLASMART Company, 373-1 Guseong-dong, Yuseong-gu, Daejeon, 305-701, Korea

(Received 30 June 2003; accepted 12 November 2003)

An atmospheric-pressure, uniform, continuous, glow plasma was produced in ambient air assisted by argon feeding gas, using a 13.56 MHz rf source. Based on the measured current–voltage curve and optical emission spectrum intensity, the plasma showed typical glow discharge characteristics, free from streamers and arc. The measured rotational and vibrational temperatures were in the range of 490 to 630 K and 2000 to 3300 K, respectively, within the operation range of argon flow rate and rf power. From the spatial measurement of total optical emission intensity, and rotational and vibrational temperatures, the plasma shows very high uniformity (over 93%) in the lengthwise direction. The plasma size for this study was 200 mm×50 mm×5 mm, although a plasma was produced in the scaled-up version of 600 mm in length, aiming for large-area plasma applications.
© *2004 American Institute of Physics.* [DOI: 10.1063/1.1639135]

Atmospheric plasma sources have recently received increased attention due to their many advantages, such as having no need for expensive vacuum equipment, being low-cost and simple systems, and easy to operate. Because of the advantages, many types of atmospheric plasma sources have been developed in a wide range of frequencies from dc to microwave, or in a short pulse. For example, a microwave and rf plasma torch, a dielectric barrier discharge (DBD), an arc plasma torch, a capacitively coupled, atmospheric-pressure plasma jet are well-known examples of atmospheric plasma sources.[1–6] In some application areas of atmospheric plasmas, especially for surface modification of large-area materials such as fabrics, polymers, or glass plates for liquid crystal displays or plasma display panels, having a large plasma volume or area with high uniformity in plasma parameters is one of the most important requirements that the plasma source should satisfy. With this motivation, a large-area, atmospheric pressure, continuous, uniform plasma source was developed and is described in this letter. It uses a DBD-type hardware arrangement in which we observed that a dielectric material covering electrodes limits the overcurrent leading to arc and assists producing a stable, uniform glow plasma at atmospheric pressure.

A schematic diagram of the discharge system is shown in Fig. 1. One of the important features of the system is its double structure with two side-discharge gaps, which provide not only volumetric but also stable plasma generation. In each side-discharge gap, an alumina plate covers each side electrode. A similar structure is placed between the central powered electrode and a bottom conductor, and the bottom-discharge gap distance was varied up to 6 mm for high-performance plasma generation. The slit-type plasma produced at each side gap assists plasma generation between the powered electrode and the bottom conductor for enlarging the plasma covering area. A typical plasma area of the device under study was 200 mm×50 mm and the height was 4–6 mm, as shown in Fig. 1(b). However, since the lengthwise dimension is an important parameter if a material for treatment is transported across the plasma, the scaled-up version with a 600 mm length produced a uniform plasma as this article was being written. By controlling the operation scheme, generation, and sustainment of plasma with bare, conducting bottom electrode was also possible. The central electrode was powered by a 13.56 MHz rf source (600 W maximum power) with a matching network. The plasma was generated in ambient air with argon gas supplied through a

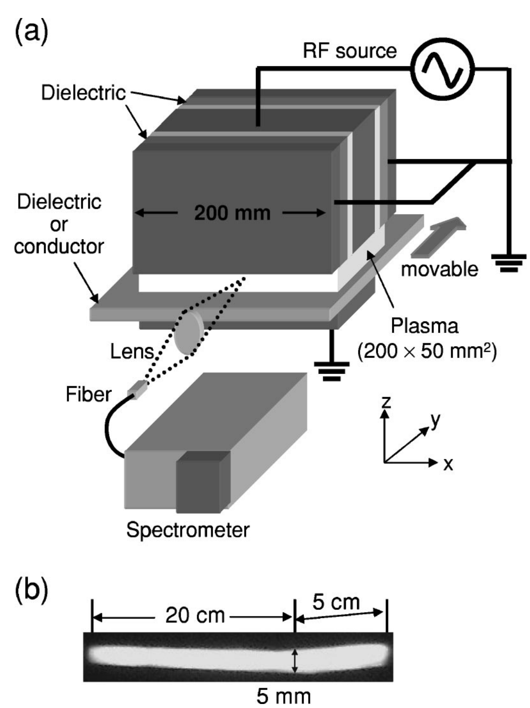

FIG. 1. (a) Schematic diagram of the experimental setup and (b) a photograph of the generated plasma.

a)Author to whom correspondence should be addressed; electronic mail: wchoe@kaist.ac.kr

Downloaded 29 Aug 2006 to 143.248.6.146. Redistribution subject to AIP license or copyright, see http://apl.aip.org/apl/copyright.jsp

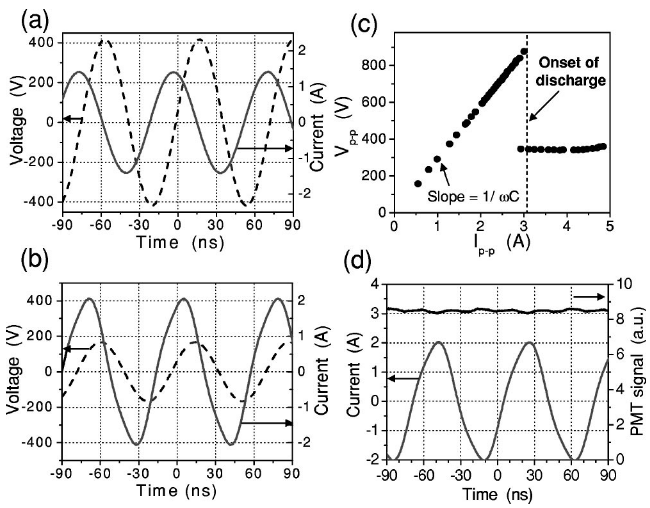

FIG. 2. (a) Current and voltage wave form in the absence of discharge and (b) in the presence of discharge. Once a discharge occurs, voltage drops, and at the same time, current increases. The phase angle between I and V also changes from $\pi/2$ to $\pi/4$, which indicates power coupling to the plasma. (c) The measured $I-V$ characteristic curve is shown to be similar to that of a typical low pressure glow discharge. (d) Total optical emission intensity as a function of time measured by a PMT. At 10 ℓpm argon flow rate and 4 mm bottom gap distance.

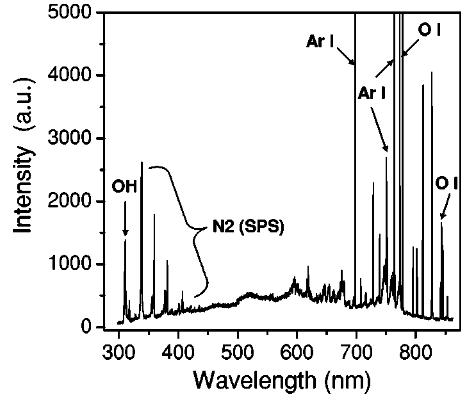

FIG. 3. A typical emission spectrum of the plasma. Due to the argon feeding gas, argon atomic lines (696.5, 763.5, 811.4, etc.) are dominant. On the other hand, the OH molecular spectrum (306–310 nm), N_2 molecular spectrum (330–425 nm), and excited oxygen atom emission lines (777 and 844 nm) are also observed due to the ambient air.

gas hole array. Introduction of argon gas flow was very important for uniform and stable plasma generation within the capability of the rf power supply used for the experiment. The electrical characteristics of the produced plasma were measured by a current (Tektronix™ TCP202) and a voltage probe (Tektronix P6015A). The visible emission spectrum from the discharge was obtained through a Chromex 250is spectrometer with a CCD detector and a photomultiplier tube (PMT).

Figures 2(a) and 2(b) show current (I) and voltage (V) measured in the absence of and in the presence of discharge, respectively. The current trace in the figure represents the current through the bottom conductor. When the discharge does not occur, the phase angle between current and voltage is $\pi/2$, indicating that the equivalent circuit of the system is purely capacitive. The capacitance of the system obtained from the slope of I and V is 32.2 pF, which is nearly equal to the capacitance of 30.8 pF calculated from the purely capacitive equivalent circuit with known dielectric size and gap distance. In the presence of discharge, however, the voltage becomes smaller but the current becomes larger. The phase angle is now $\pi/4$ due to the role of plasma as a conducting medium with low electrical resistance. It is also seen in the $I-V$ characteristic curve depicted in Fig. 2(c), where the slope of the curve that is proportional to the characteristic impedance becomes very small after the onset of discharge. At 10 ℓpm argon flow rate and 4 mm bottom gap distance, the breakdown voltage was 435 V peak. The discharge sustain voltage was about 170 V peak and remained approximately constant despite the increased current. The $I-V$ curve in Fig. 2(c) looks almost identical to that of a typical low-pressure, normal glow discharge.[7] The total optical emission intensity measured by a PMT shown in Fig. 2(d) supports the dc-like characteristic of the glow plasma. The small ripple in the PMT signal is attributed to the 13.56 MHz noise. Not only by visual observation, but also from the electrical and optical emission signals, there was no sign of the existence of either arc or filaments.

Diagnostics of the produced plasma were performed mainly by optical emission spectroscopy. As shown in a typical emission spectrum depicted in Fig. 3, excited argon atomic lines (696.5, 763.5, 811.4 nm, etc.) were dominantly observed due to the argon feeding gas. On the other hand, the OH molecular spectrum (306–310 nm), N_2 molecular spectrum (330–425 nm), and excited oxygen atom emission lines (777 and 844 nm) were also seen because the plasma was generated in ambient air. Based on the emission spectrum, rotational temperature (T_{rot}) and vibrational temperature (T_{vib}) were obtained through the analysis of OH (Ref. 8) and N_2 second positive system molecular spectrum, respectively.[9,10] Due to frequent collisions among heavy particles at atmospheric pressure, it is known that rotational temperature is nearly equal to gas temperature.[11] The vibrational temperature provides the information of the energy transfer between electrons and heavy particles, especially molecules. It was obtained by the typical Boltzmann plot method of nitrogen molecular emission spectrum. In general, the vibrational temperature lies between gas temperature and electron temperature, and shows the same tendency as electron temperature.[9,10]

The spatial uniformity of the plasma was measured because of its importance in the practical application to large area surface treatment. As shown in Fig. 4(a), the line-integrated total emission intensity that is proportional mainly to Ar I intensity was measured at each local position. It is shown to be very uniform (96.7%) along the lengthwise direction; that is, the x direction indicated in Fig. 1. Here, the spatial uniformity is defined as $1-(\max-\min)/(\max+\min)$ in percent. The spatial distributions of T_{rot} and T_{vib} are also very uniform (94.6% and 93.5%, respectively), as is seen in Figs. 4(b) and 4(c), respectively. The high uniformity of vibrational temperature suggests that the molecular excitation process occurs uniformly over the whole plasma length. The uniformity remained almost same as the input power and argon flow rate were varied. The total emission intensity measured along the side, that is, in the y direction, showed a symmetric and more or less flat profile with respect to the middle position at 25 mm, except for a small dip toward the

Downloaded 29 Aug 2006 to 143.248.6.146. Redistribution subject to AIP license or copyright, see http://apl.aip.org/apl/copyright.jsp

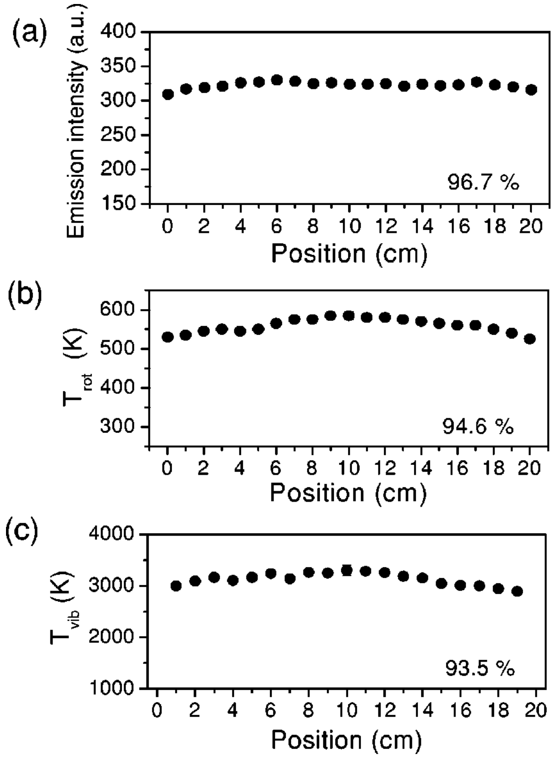

FIG. 4. Spatial distribution of (a) total optical emission intensity, (b) rotational temperature, and (c) vibrational temperature measured in the lengthwise direction. The spatial uniformity is 96.7%, 94.6%, and 93.5%, respectively. At 300 W of input power and 20 ℓpm of argon flow rate.

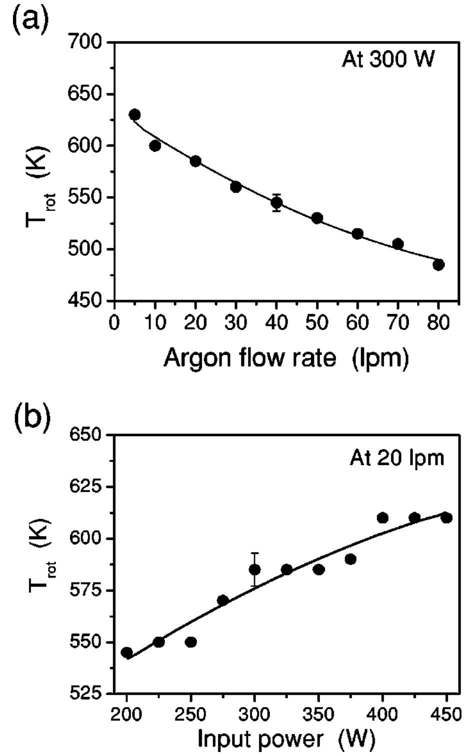

FIG. 5. Rotational temperature measured as a function of (a) argon flow rate (at 300 W), and (b) input rf power (at 20 ℓpm). T_{rot} decreases as flow rate increases due to more significant cooling by the introduced cold gas particles. T_{rot} increase as input power increases is attributed to more energy transfer from heated electrons to heavy neutrals.

middle point. This is because the effect of the slit-type plasmas formed at each side gap and pushed downward by gas flow becomes relatively small toward the middle point. However, the uniformity was still good (90%).

Figure 5 shows the measured rotational temperature as argon flow rate and input rf power were varied. It decreases as flow rate increases due to more significant cooling by the introduced cold gas particles. The T_{rot} increase as input power increases is attributed to more energy transfer from heated electrons to heavy neutral atoms. As is seen in the figure, T_{rot} ranges from 490 to 630 K depending on flow rate and power, which may be suitable for some particular applications.

In conclusion, both $I-V$ curve and optical emission signal indicate that the plasma produced at atmospheric pressure shows arc-free and streamer-free glow discharge characteristics. The measured rotational temperature and vibrational temperature suggest that the plasma can be readily applied to material surface treatment without significant thermal effect due to its low gas temperature and molecular excitation ability. The high spatial uniformity of the temperatures and optical emission intensity both in x and y directions ensures the uniform quality over the whole range of plasma covering area.

This work was partly supported by Grant No. R01-2000-00254 from the Korea Science and Engineering Foundation.

[1] M. Moisan, J. Hubert, J. Margot, G. Sauvé, and Z. Zakrzewski, *Microwave Discharge: Fundamentals and Applications*, edited by C. M. Ferreira and M. Moisan (Plenum, New York, 1992), Chap. 1.
[2] S. Y. Moon, W. Choe, H. S. Uhm, Y. S. Hwang, and J. J. Choi, Phys. Plasmas **9**, 4045 (2002).
[3] J. Park, I. Henins, H. W. Hermann, and G. S. Selwyn, J. Appl. Phys. **89**, 15 (2001).
[4] F. Massines, A. Rabehi, P. Descomps, R. Ben Gadri, P. Ségur, and C. Mayoux, J. Appl. Phys. **83**, 2950 (1998).
[5] M. Šimor, J. Ráhel', P. Vojtek, M. Černák, and A. Brablec, Appl. Phys. Lett. **81**, 2716 (2002).
[6] Y. B. Guo and F. C. N. Hong, Appl. Phys. Lett. **82**, 337 (2003).
[7] H. Conrads and M. Schmidt, Plasma Sources Sci. Technol. **9**, 441 (2000).
[8] S. Y. Moon and W. Choe, Spectrochim. Acta, Part B **58**, 297 (2003).
[9] S. D. Popa, J. Phys. D **29**, 411 (1996).
[10] G. Herzberg, *Molecular Spectra and Molecular Structure: 1. Spectra of Diatomic Molecules*, 2nd ed. (Van Nostrand, Princeton, 1964).
[11] A. Czernichowski, J. Phys. D **20**, 559 (1987).

Downloaded 29 Aug 2006 to 143.248.6.146. Redistribution subject to AIP license or copyright, see http://apl.aip.org/apl/copyright.jsp